Journal of Low Temperature Physics, Vol. 99, Nos. 5/6, 1995

Bound States of ^{3}He in ^{3}He-^{4}He Mixture Films

Eugene Bashkin

Department of Physics and Material Sciences Center, Phillips University, 35032 Marburg, Germany, and Kapitza Institute for Physical Problems, 117334 Moscow, Russia

Nicolas Pavloff and Jacques Treiner

Division de Physique Théorique, Institut de Physique Nucléaire, F-91406 Orsay Cedex, France*

(Received July 15, 1994; revised December 22, 1994)

^{3}He atoms dissolved in superfluid ^{4}He may form dimers $(^3He)_2$ in two-dimensional (2D) geometries. We study dimer formation in films of dilute ^{3}He-^{4}He mixture. After designing a schematic ^{3}He-^{4}He interaction potential we calculate the dimer binding energy for various substrates. It is shown that ^{3}He impurity states localized near the substrate give rise to the largest magnitudes of the binding energies.

1. INTRODUCTION

^{3}He atoms dissolved in bulk ^{4}He have always been considered an ideal system for testing the Landau approach describing the macroscopic properties of quantum fluids in terms of elementary excitations (quasiparticles).[1] At low enough temperatures one can neglect the contribution of the excitations pertaining to superfluid ^{4}He (phonons and rotons). The system is then described in terms of an interacting gas of ^{3}He quasiparticles imbedded in the uniform background of superfluid ^{4}He. A bare quasiparticle has a particle-like energy spectrum[2] with an effective mass larger than the bare mass. The quasiparticle interaction at long distances is the bare ^{3}He-^{3}He interatomic interaction renormalized by a phonon-induced term.[3] At small distances a strong repulsive core is predominant. However, the overall effect turns out to be attractive, as was demonstrated on the basis of theoretical calculations[4,5] and experimental data[6,7] on the s-wave scattering length a ($a < 0$).

*Unité de Recherche des Universités Paris XI et Paris VI associée au CNRS.

0022-2291/95/0600-0659$07.50/0

Despite the fact that the effective attraction between two ^{3}He quasiparticles is too weak to lead to a bound state in the bulk, such a bound state—a $(^3\text{He})_2$ dimer—should certainly exist in helium systems with reduced dimensionality.[8,9] It is well known that in one and two dimensions any attractive potential satisfying the perturbation theory criterion gives rise to a bound state (see e.g., Ref. [10]). The result does not apply, however, in the case of a nonperturbative potential like the ^{3}He-^{3}He interaction, with a strong repulsion at short distances. Nevertheless, one can rigorously prove that spinless $(^3\text{He})_2$ dimer must exist in quasi-2D and quasi-1D geometries (like films and narrow capillaries of ^{4}He) provided a is negative and the characteristic scale of confinement of the ^{3}He atoms is much larger than the interaction range—which is of the order of $|a|$—(see [9] and appendix A). When the system is cooled down to temperatures lower than the corresponding binding energy, the single impurity quasiparticles form $(^3\text{He})_2$ Bose-dimers, and the Fermi component of ^{3}He is replaced by a new Bose quantum fluid of $(^3\text{He})_2$ of reduced dimensionality. This phenomenon should strongly affect the macroscopic properties of dilute mixtures resulting in an extra superfluid transition, new features of the phase diagram, anomalous sound absorption, etc.[8] This is the reason why calculating the binding energy is the main issue in the theory of dimerized ^{3}He-^{4}He solutions. To be specific we will concentrate on dilute ^{3}He-^{4}He mixtures in various 2D geometries (i.e., in films on various substrates).

In ^{4}He films, ^{3}He impurities are localized in the direction normal to the substrate over a characteristic width w which can be much smaller than the film thickness. When extrapolated to small w (of the order of a few atomic layers) the theory of Ref. [8, 9] provides an estimate for the binding energy which seems to be quite attainable for experimental studies. However, it is difficult to assess the accuracy of such an estimate because the theory in question certainly does not hold in such restricted geometry, i.e., in a real 2D situation (when $w \sim a$). In a pure 2D case one cannot a priori be sure if a bound state of two ^{3}He atoms exists at all. Therefore, calculating the binding energy for various film thickness and different substrates may provide direct clue on which experimental conditions are best suited for the detection of $(^3\text{He})_2$ dimers. Such calculations are the primary goal of this paper. Here we focus on two cases where ^{3}He impurities adopt a 2D configuration:

(i) The Andreev states of ^{3}He at the free surface of ^{4}He (see [11, 12, 13] and references therein).

(ii) The ^{3}He states localized at the interface between a ^{4}He film and the substrate, as predicted in [14, 15].

Case (ii) seems particularly favorable for the creation of dimers because ^{3}He quasiparticles near the substrate have a large effective mass (due to the higher ^{4}He density) and a narrow wave-function (localized within the first ^{4}He liquid layer). The localization length (the width of the wave function in the direction across the film) is of the order of a few angströms. In Sec. 2 some possible realizations of a quasi-2D ensemble of ^{3}He impurities in superfluid ^{4}He films on various substrates are reviewed. In Sec. 3 we derive a schematic ^{3}He-^{3}He interaction and then evaluate in Sec. 4 the corresponding $(^3\mathrm{He})_2$ binding energy. We give our concluding remarks in Sec. 5.

2. ^{3}HE IMPURITIES IN ^{4}HE FILMS

We assume in the following that inhomogeneities of the substrate in the $x-y$ plane parallel to the surface play a negligible role and we impose translational invariance on the helium densities (^{3}He and ^{4}He). This does not imply that possible corrugation of the surface is neglected. Indeed, in that case, ^{4}He atoms will certainly fill the dips of the surface until it is more or less flat; the effective substrate to be considered is then a mixture of the original substrate and these helium atoms, the effect of which is to weaken the potential.

The first question to address is to determine the state of liquid helium on a given substrate. The different situations to expect, as a function of increasing attractive strength of the substrate potential, are the following: non wetting, wetting with prewetting,[16] and solidification of one or two layers. We limit our study to cases where no solid layer forms near the substrate: there is a clear qualitative change of ^{3}He impurity states when ^{4}He solidifies; the ^{3}He atoms occupy substitutional states in solid ^{4}He and move through the lattice via tunneling processes (see e.g., Ref. [17]). Our continuous description of the solid misses this phenomenon, since the coupling of ^{3}He atoms with the ^{4}He matrix is represented here through a density dependent ^{3}He effective mass fitted on properties of liquid mixtures (see details in Ref. [14]).

Hence, in order to specify the validity of our approach we need a criterion assigning a solid or liquid character to each of the first ^{4}He layers. This has been done in Ref. [18] where different substrates were characterized by their interaction with helium through two coefficients C_3 and D

$$V_{\mathrm{sub}}(z)=\frac{4}{27D^2}\left(\frac{C_3}{z^3}\right)^3-\frac{C_3}{z^3} \tag{1}$$

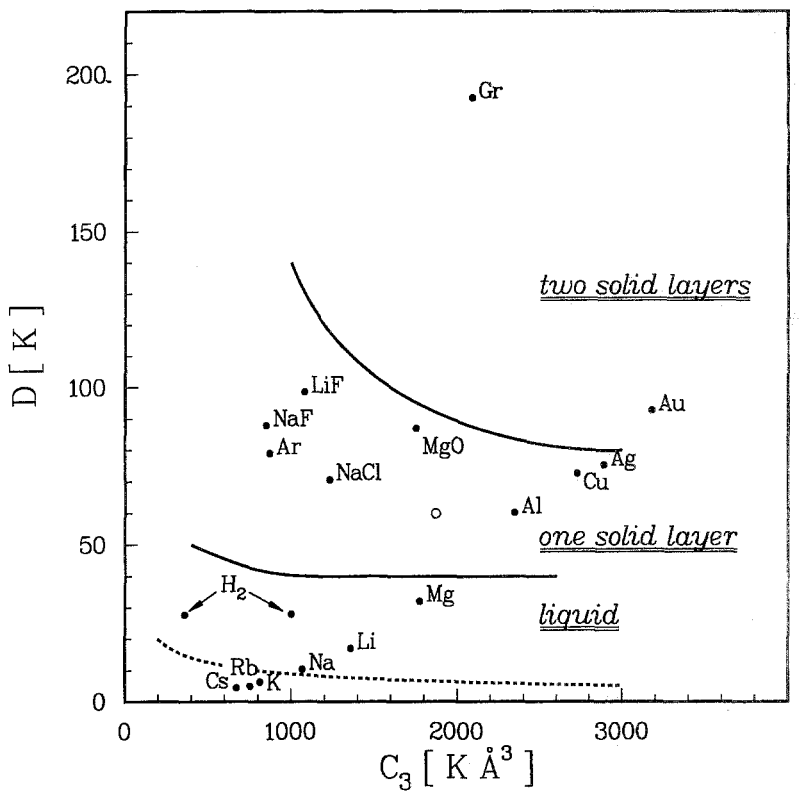

Fig. 1. Phase diagram of ^{4}He on various substrates at zero temperature (from [18]). The dotted line is the wetting line.[16]

Here D is the depth of the attractive part of $V_{sub}(z)$ and C_3 characterizes the van der Waals tail. According to Ref. [18] one can draw in the $C_3 - D$ plane the lines corresponding to solidification of the first and second layer (see Fig. 1). For completeness, we have also reproduced, from Ref. [16], the line separating the non-wetting region from the wetting one. Notice that the criterion used in [18] is only approximate and also that there are large uncertainties in the parameters of the potentials (up to $\sim 30\%$ on D).[19] As an extreme case, for hydrogen the value $C_3 = 1000$ KÅ^3 extracted from different experiments (see [20] and references therein) is significantly larger than the theoretical value of 360 KÅ^3 from Ref. [19]. So, the predictions are uncertain for cases close to a line: it may well be that the first layer does solidify on Mg, and that the second layer solidifies on MgO, Cu, and Ag.

We now come to the ^{3}He impurity states. Calculations were performed, as in Ref. [14], in the limit of one ^{3}He atom. When considering finite

^{3}He coverage, each state generates a 2D Fermi disc, characterized by a 2D Fermi momentum. Also, through self-consistency, the ^{4}He profile, the ^{3}He average field—and consequently the single particle states—depend on the ^{3}He coverage (see Ref. [13] for a study of finite ^{3}He coverage on the ^{4}He bulk surface). We shall neglect these effects in the following discussion, which is valid for small ^{3}He coverage only.

Variation of the density functional with respect to the impurity wave function ϕ leads to the following equation

$$-\frac{d}{dz}\left(\frac{\hbar^2}{2m^*(z)}\frac{d\phi}{dz}\right)+U_{\text{ext}}(z)\,\phi(z)=\varepsilon\,\phi(z) \tag{2}$$

$U_{\text{ext}}(z)$ is the ^{3}He mean field, see Ref. [14]. It comprises a term due to ^{3}He-^{4}He interaction plus the substrate potential V_{sub}. The density-dependent effective mass is parametrized as:

$$\frac{\hbar^2}{2m^*(\mathbf{r})}=\frac{\hbar^2}{2m_3}\left(1-\frac{\bar{\rho}_4(\mathbf{r})}{\rho_{4c}}\right)^2 \tag{3}$$

where $\rho_{4c}=0.062$ Å^{-3} and $\bar{\rho}_4(\mathbf{r})$ is the local ^{4}He density averaged over a sphere of radius 2.38 Å (see Ref. [14]). This parametrization is fitted to the pressure dependence of the ^{3}He effective mass in bulk liquid ^{4}He.[21]

Then the effective mass M^* of the ^{3}He impurity in a given state is defined by:

$$\frac{\hbar^2}{2M^*}=\int_{-\infty}^{+\infty}dz\,\frac{\hbar^2}{2m^*(z)}\phi^2(z) \tag{4}$$

One can check that an energy close to that obtained through Eq. (2) can be recovered from the effective hamiltonian containing the constant effective mass M^*

$$H=\frac{\mathbf{p}^2}{2M^*}+U_{\text{ext}}(z) \tag{5}$$

where U_{ext} is the effective ^{3}He potential appearing already in Eq. (2).

Fig. 2 shows the results for the ^{4}He density profile and the ^{3}He wave function near a Cs and a Li surface. Numerical results for other substrates are displayed in Table 1. The existence of 2D ^{3}He states near a weakly binding surface, although somewhat counter-intuitive, appears as a general feature of these interfaces.

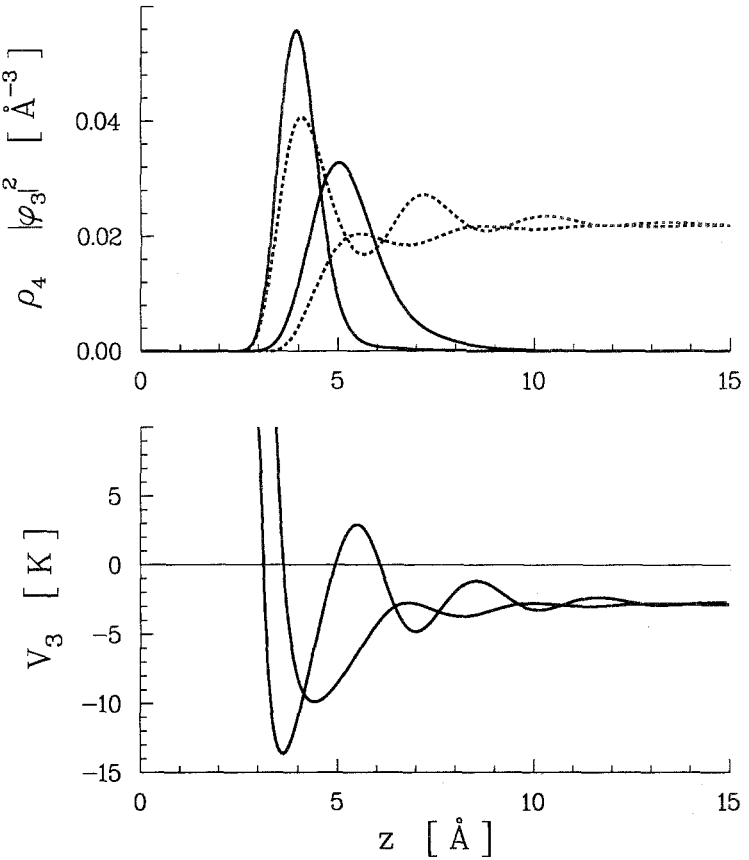

Fig. 2. ^{4}He liquid density (dotted line), ^{3}He substrate state wave-function (with arbitrary units) and ^{3}He average field on a Cs substrate (less attractive) and Li substrate (more attractive).

The physics behind this feature is best understood by considering a Lekner approach to the problem. In this variational method, the ansatz for the wave function Ψ of $N-1$ ^{4}He atoms and one ^{3}He atom is taken as

$$\Psi(1, 2,..., N) = \phi(1)\, \Psi_0(1, 2,..., N) \tag{6}$$

where ϕ denotes the wave function of the impurity and Ψ_0 the ground state wave function of N ^{4}He atoms. Variation of the average energy of the

TABLE I

Energy (ε), effective mass (M^*) and half-width (w) of the ^{3}He impurity state on various substrates and for the Andreev state. In the case of H_2, the value $C_3 = 1000$ KÅ^3 extracted from different experiments[20] is different from the theoretical value of 360 KÅ^3.[19]

Substrate	C_3 [KÅ^3]	D [K]	ε [K]	M^*/m_3	w [Å]
Cs	673	4.4	−4.74	1.51	2.0
Rb	754	5.0	−4.23	1.78	1.9
K	812	6.3	−4.15	1.84	1.8
Na	1070	10.4	−4.04	2.02	1.4
Li	1360	17.1	−4.17	2.28	1.2
Mg	1780	32.0	−5.00	2.90	0.9
H_2	360	28.0	−5.51	2.41	0.9
	1000	28.0	−5.00	2.61	0.9
^{4}He free surface			−5.20	1.35	3.6

system with respect to ϕ results in a one-body Schrödinger equation (without effective mass effects)

$$-\frac{\hbar^2}{2m_3}\phi''(z) + U^L_{\text{ext}}(z)\,\phi(z) = \varepsilon\,\phi(z) \tag{7}$$

where U^L_{ext} is an external field due to both the substrate and the ^{4}He environment,

$$U^L_{\text{ext}}(z) = \frac{\hbar^2}{2m_3}\frac{\phi_4''(z)}{\phi_4(z)} + \left(\frac{m_4}{m_3} - 1\right)\tau_4(z) + \mu_4 + V_{\text{sub}}(z) \tag{8}$$

Here $\phi_4(z) = \sqrt{\rho_4(z)}$, μ_4 is the ^{4}He chemical potential, $\tau_4(z)$ the kinetic energy density in the ^{4}He ground state and $V_{\text{sub}}(z)$ is the substrate potential.

In the case of a free surface originally considered by Lekner, $V_{\text{sub}} = 0$; then Eq. (8) provides a mechanism for the formation of the pocket of potential at the surface: the kinetic energy density τ_4 goes to zero faster than the term in ϕ_4''. For a numerical study, one assumes that $\tau_4(z)$ can be parametrized in term of the local density $\rho_4(z)$. The simple following form was proposed in Refs. [22, 24]

$$\tau_4(\mathbf{r}) = \tau_0\left(\frac{\rho_4(\mathbf{r})}{\rho_0}\right)^n - \frac{\hbar^2}{2m_4}\frac{\Delta\phi_4(r)}{\phi_4(r)} \tag{9}$$

where the value $\tau_0 = 13.3$ K is chosen so that the binding energy of a ^{3}He atom in the bulk ^{4}He is -2.8 K; ρ_0 is the saturation density of liquid ^{4}He

and the value $n = 1.76$ has been related to the excess volume parameter and the compressibility in dilute ^{3}He-^{4}He mixtures.[22]

The effective potential U_{ext}^L resulting from the Lekner theory for a film of 0.6 Å^{-2} on a Mg substrate in shown in Fig. 3. The average field U_{ext} obtained using the density functional theory is shown for comparison. One sees that the Lekner field is slightly more attractive at the surface; the corresponding energy of the Andreev state is found to be -5.24 K (using the bare ^{3}He mass) whereas the density functional result is -5.27 K, with $M^* = 1.34\, m_3$ (the experimental result being $\varepsilon = (-5.02 \pm 0.03)$ K and $M^*/m_3 = 1.45 \pm 0.1$, see Ref. [23]). Close to the substrate the average fields given by the two theories show similar qualitative behaviour, with attractive wells in correspondence with the oscillations of the ^{4}He density. The Lekner field is more attractive than the density functional one, and leads to $\varepsilon = -14.1$ K (using the bare mass), while the density functional theory gives $\varepsilon = -5$ K, with $M^* = 2.9 m_3$. We believe that the density functional

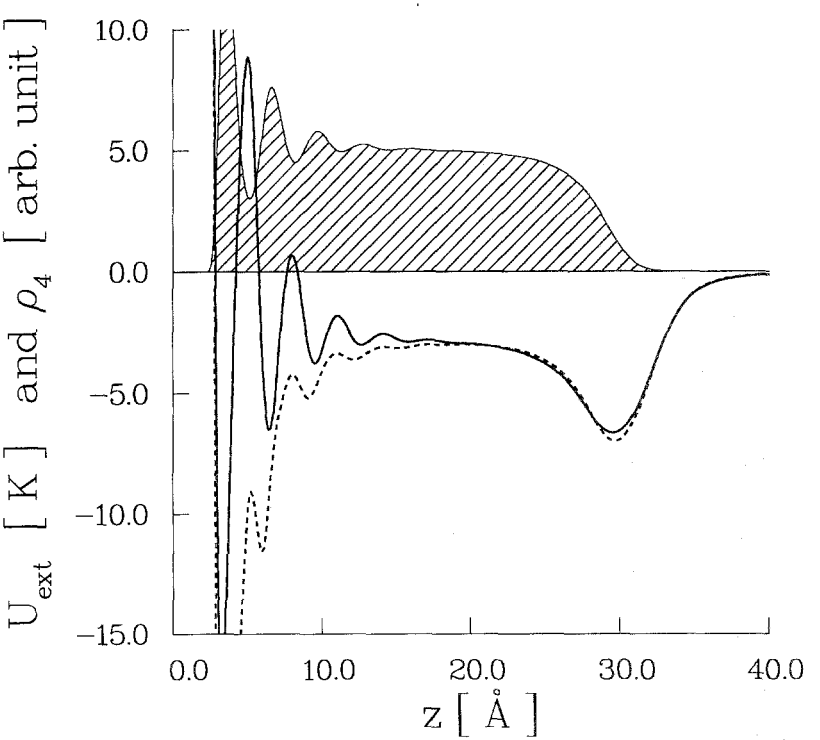

Fig. 3. ^{4}He film (0.6 atoms per Å^2, i.e., 7.7 atomic layers) and ^{3}He mean field on a magnesium substrate. The solid line is the density functional mean field U_{ext} and the dashed line is the result of Lekner's approach U_{ext}^L.

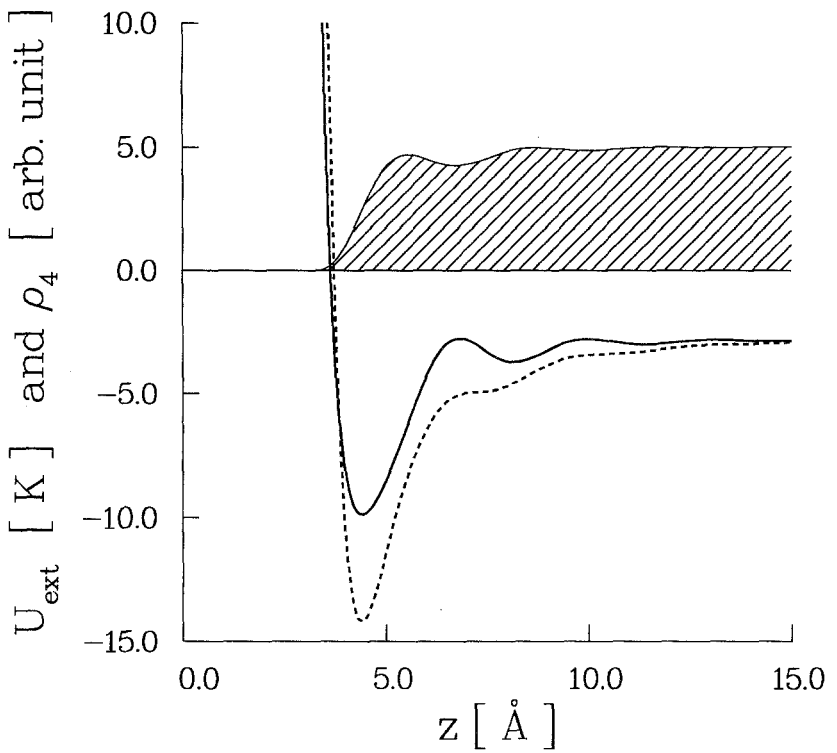

Fig. 4. Infinite ^{4}He film and ^{3}He mean field on a cesium substrate. The solid line is the Density Functional mean field U_{ext} and the dashed line is the result of Lekner's approach U_{ext}^L.

results are more reliable, since the model is fitted to a larger number of bulk mixture properties. The case of a semi-infinite liquid in contact with a Cs substrate is shown in Fig. 4. The Lekner value is $\varepsilon = -6.3$ K, compared to the density functional value $\varepsilon = -4.74$ K, with $M^* = 1.51 m_3$.

Note that the Lekner result could be improved by a modification of the parametrisation of Eq. (9). Here we only want to point out that substrate states are not specific to the density functional method, but emerge from the general features of the substrate-helium interface.

To summarize, we stress here is that the mechanism by which an Andreev state is generated at the free surface of liquid helium is also operating at the liquid substrate interface. On a free surface, a ^{3}He impurity is bound by 5 K (Andreev state), i.e., by 2.2 K more than in the bulk. Now a weak binding substrate perturbs the energetics of the free surface in two competitive ways, namely: i) the wall produces a readjustment of the ^{4}He density profile, which reduces the width of the ^{3}He wave function, and this tends to increase the energy of the state (to make it less bound); ii)

however the attractive substrate potential acts on the ^{3}He atom also and tends to decrease the energy of the ^{3}He state. Clearly, if the perturbation is small enough, the gap of 2.2 K between the unperturbed surface energy and the bulk energy will not vanish, therefore a bound state has to remain at the liquid-wall interface.

That the argument remains valid also in the case of Mg, wich produces quite a marked layering of the fluid, may seem surprising. Whether we reach in that case the limit of the model remains to be seen by comparing with more microscopic calculations or with experiment.

As discussed in [14] the existence of a substrate state allows one understand some unexplained temperature dependence of third sound velocities reported in Ref. [25]. Several experimental tests of its existence were proposed in Ref. [14, 15]. Recently, experimental evidence was reported that ^{3}He impurities have a bound state at the ^{4}He liquid-solid interface,[26] with a binding energy in fair agreement with the prediction of Ref. [15]. In the following we focus on one of the most exciting consequences: the possible formation of $(^3\text{He})_2$ dimers with a sizeable binding energy.

3. A SCHEMATIC ^{3}HE-^{3}HE INTERACTION

The next step in evaluating the dimer binding energy is to choose a sensible effective interaction between the ^{3}He quasiparticles. The requirements are three-fold: (1) the long range attraction is the bare term reduced by a factor α^2 where α is the excess volume parameter in ^{4}He (see [3, 27] and below); (2) as mentioned in the introduction, the short distance term is repulsive and equal to the bare potential; (3) the effective potential should reproduce the s-wave scattering length a of ^{3}He in ^{4}He ($a \simeq -0.97$ Å, see Ref. [6]).

Let us start with the first requirement; it will lead us to postulate a generic form for the effective potential. Our derivation of the energy of two ^{3}He atoms imbedded in ^{4}He is patterned on the approach of Ref. [27]. We consider two ^{3}He atoms located at points $\mathbf{r}_1$ and $\mathbf{r}_2$. Atom i ($i=1, 2$) occupies a volume Ω_3 centered at $\mathbf{r}_i$ (we denote it as $\Omega_3[\mathbf{r}_i]$) of which the ^{4}He atoms are expelled (see Fig. 5). So, if the total volume of the sample is Ω, the ^{4}He's will occupy a volume $\Omega' = \Omega - \Omega_3[\mathbf{r}_1] - \Omega_3[\mathbf{r}_2]$. If ρ_4 is the mean ^{4}He density, then one can consider that each ^{4}He atom occupies a volume $\Omega_4 = 1/\rho_4$ and the excess volume parameter is by definition

$$\alpha = \frac{\Omega_3 - \Omega_4}{\Omega_4} \tag{10}$$

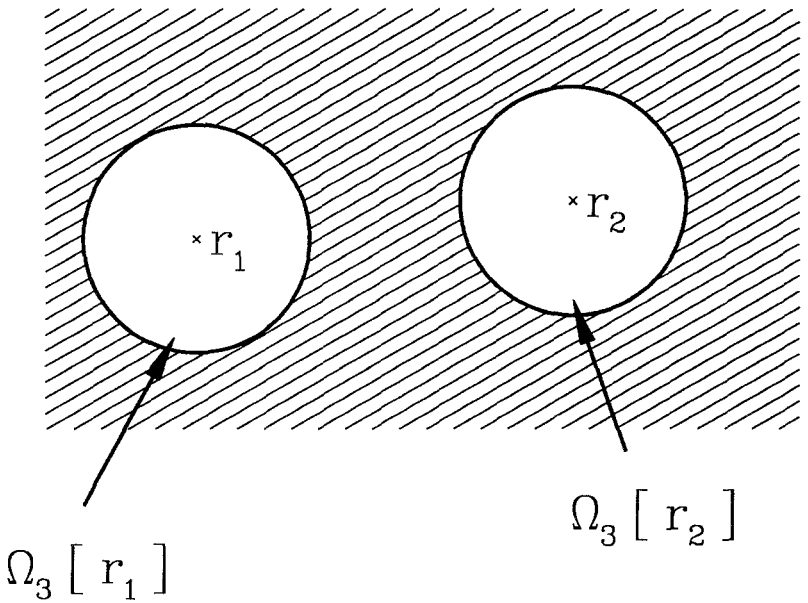

Fig. 5. Schematic representation of the behaviour of two ^{3}He atoms situated at points $\mathbf{r}_1$ and $\mathbf{r}_2$ in bulk liquid ^{4}He. Atom i ($i=1, 2$) occupies a volume $\Omega_3[\mathbf{r}_i]$ of which the ^{4}He's are expelled (see the text). The shaded zone represents the volume occupied by liquid ^{4}He.

The total potential energy of the system is

$$E = E_{33} + E_{34} + E_{44} \tag{11a}$$

with obvious notations (for instance E_{34} is due to the ^{3}He-^{4}He interaction). E can be separated into a constant (i.e., position independent) term C^{st} plus a term which is an effective ^{3}He-^{3}He potential:

$$E = C^{st} + V_{eff}(|\mathbf{r}_1 - \mathbf{r}_2|) \tag{11b}$$

The separation (11b) is made unambiguous by imposing that V_{eff} goes to zero at large distance (when the two ^{3}He impurities are far apart).

Let us now study the contributions of E_{33}, E_{34} and E_{44} to the effective potential V_{eff}.

If two helium atoms interact via the bare Lennard-Jones potential V_{LJ}, E_{33} is simply

$$E_{33} = V_{LJ}(|\mathbf{r}_1 - \mathbf{r}_2|) \tag{12}$$

where the explicit form of V_{LJ} is

$$V_{LJ}(r) = 4v_0 \left[\left(\frac{\sigma}{r}\right)^{12} - \left(\frac{\sigma}{r}\right)^{6} \right] \tag{13}$$

with $v_0 = 10.22$ K and $\sigma = 2.556$ Å.

The cross term E_{34} is

$$E_{34} = \int_{\Omega'} V_{LJ}(|\mathbf{r}_1 - \mathbf{r}|) \frac{d^3r}{\Omega_4} + \int_{\Omega'} V_{LJ}(|\mathbf{r}_2 - \mathbf{r}|) \frac{d^3r}{\Omega_4} \tag{14}$$

In the r.h.s. of (14) the two integrals are equal. Let us focus on the first one for instance. The integration domain can be separated into two contributions: $\Omega' = (\Omega - \Omega_3[\mathbf{r}_1]) - \Omega_3[\mathbf{r}_2]$. The first subdomain describes the energy due to the introduction of atom 1 alone in the ^{4}He matrix. It corresponds to the "dressing" of the bare ^{3}He particle and plays no role in the quasiparticle interaction (i.e., it does not depend on $|\mathbf{r}_1 - \mathbf{r}_2|$ and can be included in the constant term of Eq. (11b)). The second subdomain describes the interaction of particle 1 with fictitious ^{4}He atoms occupying $\Omega_3[\mathbf{r}_2]$ and brings a contribution to V_{eff}, since it depends of the respective position of the ^{3}He impurities. Hence E_{34} contributes to $V_{\text{eff}}(|\mathbf{r}_1 - \mathbf{r}_2|)$ with the following term (the factor 2 comes from the sum of the two equal integrals appearing in (14)):

$$E_{34} \rightsquigarrow -2 \int_{\Omega_3[\mathbf{r}_2]} V_{LJ}(|\mathbf{r}_1 - \mathbf{r}|) \frac{d^3r}{\Omega_4} \simeq -2 \frac{\Omega_3}{\Omega_4} V_{LJ}(|\mathbf{r}_1 - \mathbf{r}_2|) \tag{15}$$

In the last term of (15) we have replaced the integral by an approximate form valid only if $|\mathbf{r}_1 - \mathbf{r}_2|$ is large compared with the characteristic radius of Ω_3. If not, the dressing of the quasiparticles might affect one another (see below).

The term E_{44} is

$$E_{44} = \frac{1}{2} \iint_{\Omega' \times \Omega'} V_{LJ}(|\mathbf{r} - \mathbf{r}'|) \frac{d^3r}{\Omega_4} \frac{d^3r'}{\Omega_4} \tag{16}$$

As above, the integration domain can be separated into several subdomains. The position dependent part of E_{44} gives a contribution to V_{eff} which represents the interaction of fictitious ^{4}He atoms occupying the volumes $\Omega_3[\mathbf{r}_1]$ and $\Omega_3[\mathbf{r}_2]$

$$E_{44} \rightsquigarrow \iint_{\Omega_3[\mathbf{r}_1] \times \Omega_3[\mathbf{r}_2]} V_{LJ}(|\mathbf{r} - \mathbf{r}'|) \frac{d^3r}{\Omega_4} \frac{d^3r'}{\Omega_4} \simeq \left(\frac{\Omega_3}{\Omega_4}\right)^2 V_{LJ}(|\mathbf{r}_1 - \mathbf{r}_2|) \tag{17}$$

As in (15) the last term of Eq. (17) is a long distance approximation.

Gathering the contributions (12, 15, 17) we see as stated in the beginning of this section that the long range quasi-particle interaction is equal to the bare interaction reduced by a factor α^2. Essentially the same result was obtained in [3] using thermodynamical arguments in momentum space. In the terminology of Ref. [3] the contribution of $E_{33}+E_{34}$ would correspond to the direct part of the effective interaction and E_{44} would give the phonon-induced term. Of course, derivations based on excluded volume arguments such as in [3] or as presented here (from [27]) are only valid for long wavelengths, i.e., for large distances between the ^{3}He atoms. Working in real space has the advantage of providing a simple way to build an effective interaction sensible also at short distance: if the two atoms get closer one can mimic the interaction of the dressed particles by introducing a correlation term $g(r)$ describing phenomenologically effects such as the disturbance of the ^{4}He cloud around a ^{3}He atom by the other particle. We choose for the correlation function the following form ($r=|\mathbf{r}_1-\mathbf{r}_2|$):

$$g(r)=\exp\left\{-\left(\frac{r_c}{r}\right)^5\right\} \tag{18}$$

Then the contribution of E_{34} to V_{eff} is approximatively given by its long range approximation (the r.h.s. of (15)) multiplied by a factor $g(r)$. Similarly the contribution of E_{44} is multiplied by $g^2(r)$, leading to a total effective interaction

$$V_{\text{eff}}(r)=[1-(1+\alpha)\,g(r)]^2\,V_{LJ}(r) \tag{19}$$

The short range and long range behavior of the effective interaction (19) follow the requirements (1) and (2) stated in the beginning of this section. Requirement (3) will be fulfilled by a correct choice of the free parameter r_c in (18). The value $r_c=3.684$ Å gives the correct s-wave scattering length $a=-0.97$ Å (see Ref. [6]). The potential V_{eff} is shown on Fig. 6 where it is compared to the bare Lennard-Jones interaction. We have checked that working with a more realistic bare interaction such as the Aziz potential [28] does not affect the qualitative picture presented below. Also the potential in films should be different from the bulk interaction: at the free surface for instance, ripplon—and not phonon—exchange should dominate the long range behaviour. Or equivalently, the excess volume parameter should be replaced by an "excess surface parameter". We will not discuss this effect in the paper.

In order to test the sensibility of the final results to the effective interaction we designed another potential $\tilde{V}_{\text{eff}}$ having the required properties

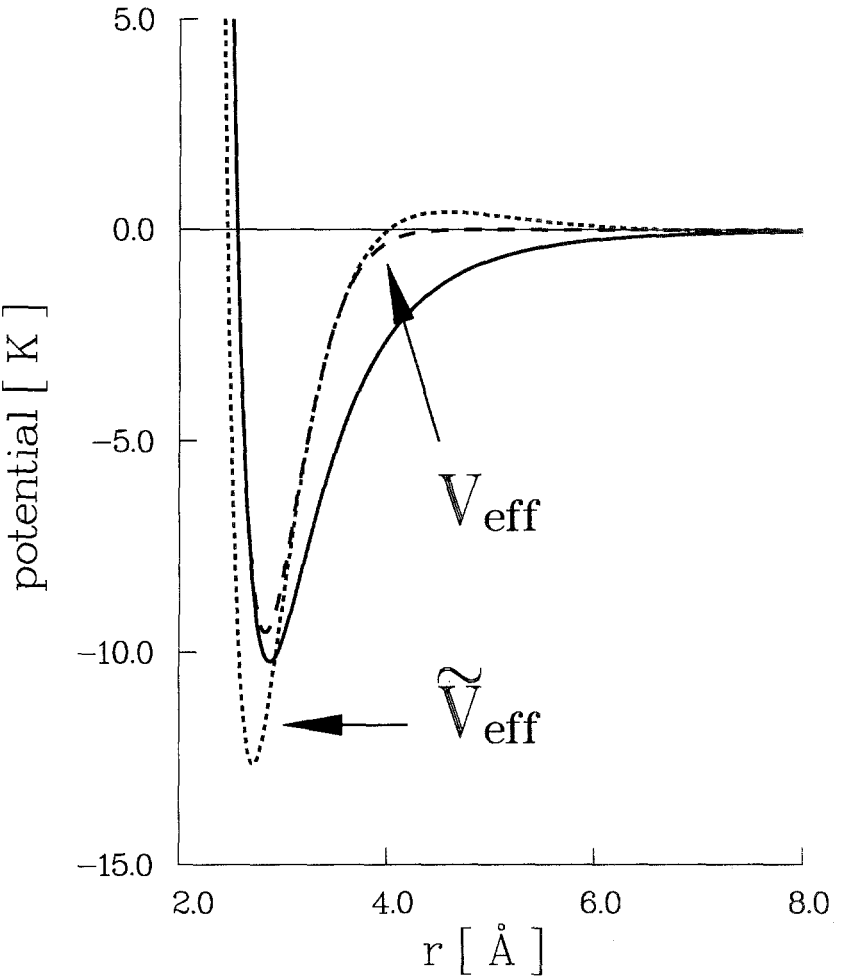

Fig. 6. ^{3}He interaction potentials. The solid line represents the bare Lennard-Jones potential V_{LJ}, the dashed lines represent the effective potentials V_{eff} (long dashes) and $\tilde{V}_{\text{eff}}$ (short dashes).

and roughly imitating at long range the potential derived by Owen using the hypernetted chain approximation.[29] The potential was chosen to be:

$$\tilde{V}_{\text{eff}}(r) = 4v_0 \left[\left(\frac{\sigma}{r}\right)^{12} - \alpha^2 \left(\frac{\sigma}{r}\right)^{6} - C\left(\frac{\sigma}{r}\right)^{7} \cos\left(2\pi \frac{r-\sigma}{R}\right) \right] \tag{20}$$

This form obviously fulfills requirements (1) and (2) above. The parameters C and R are chosen so that $\tilde{V}_{\text{eff}}$ has a zero at $r = 4$ Å as in

Owen's results (this imposes $R = 5.776$ Å) and that the s-wave scattering length has the correct value (this fixes $C = 1.145$). The corresponding $\tilde{V}_{\text{eff}}$ is plotted on Fig. 6. Note that the potential of Ref. [29] is much deeper than $\tilde{V}_{\text{eff}}$ (it has a minimum at approximatively 19 K) and this would favour dimer's creation. On the other hand Owen uses no effective mass and this goes against binding. Hence we cannot directly compare our approach with the one of Ref. [29]; Owen's work is taken here only as an inspiration for designing a new potential in order to test the sensitivity of our results to the effective ^{3}He-^{3}He interaction.

4. $(^3\text{HE})_2$ DIMERS

The Hamiltonian describing two ^{3}He quasiparticles in the film has the form:

$$H = \frac{\mathbf{p}_1^2}{2M^*} + \frac{\mathbf{p}_2^2}{2M^*} + V_{\text{eff}}(|\mathbf{r}_1 - \mathbf{r}_2|) + U_{\text{ext}}(z_1) + U_{\text{ext}}(z_2) \tag{21}$$

where U_{ext} is the ^{3}He mean field due to both the substrate and the ^{4}He film (such as shown on Figs. 2, 3 and 4) and M^* the ^{3}He effective mass for the surface (Andreev) or substrate state (cf. Table I). It should be pointed out that the ^{3}He particles described by Eq. (21) may, in general, be in two different localized states in the z-direction, i.e., may belong to two different 2D continua. In this case the effective masses of both quasiparticles in the Hamiltonian (21) may be quite different. As explained earlier we restrict ourselves to considering the case of two ^{3}He particles in the same state concerning motion along the z-axis, since it provides the largest binding energy. In Eq. (21) and in the following V_{eff} is used as a generic notation valid for both potentials V_{eff} and $\tilde{V}_{\text{eff}}$. The description might in general be improved by phenomenoligically introducing a ^{3}He concentration-dependent effective mass M^* within the local density functional approach to ^{3}He-^{4}He mixtures.[13] However the uncertainty in evaluating the dimer binding energy are such that this correcting term goes beyond the accuracy of the theory (see below).

We make the following ansatz for the wave function of the two ^{3}He atoms:

$$\Psi(\mathbf{r}_1, \mathbf{r}_2) = \frac{1}{2\pi} e^{i\mathbf{K}_{||} \cdot \mathbf{R}_{||}} \chi(\mathbf{r}_{||})\, \phi(z_1)\, \phi(z_2) \tag{22}$$

Eq. (22) describes two fermions with opposite spins. $\mathbf{R}_{||}$ is the center of mass coordinate in the (x, y) plane. For a dimer at rest (as we consider

in the following) the corresponding momentum $\mathbf{K}_{||}$ is zero. The variable $\mathbf{r}_{||}$ is the relative coordinate in the plane. We have separated the (x, y) and z direction. The functions $\phi(z_1)$ and $\phi(z_2)$ describe the motion along the z-axis. We assume (which is exact to the first order of perturbation theory) that they are of the type shown on Fig. 2, not being affected by the coupling between the two atoms. So the main point here is that the interaction between ^{3}He atoms just slightly disturbs the motion in the z-direction but entirely changes the relative motion in the plane and leads to a bound state. In other words a perturbation theory can be applied for describing the normal motion only but the transverse dynamics of particles should be determined from the exact Schrödinger equation. In practice this means that one has to solve the 2D Schrödinger equation with a potential averaged over the unperturbed wave functions of ^{3}He quasiparticles in the z coordinate. The function ϕ is determined by the solution the equation:

$$\left[\frac{p_z^2}{2M^*} + U_{\text{ext}}(z)\right] \phi(z) = \varepsilon\, \phi(z) \tag{23}$$

where p_z is the z component of the momentum ($z = z_1$ or z_2):

$$\frac{\mathbf{p}_1^2}{2M^*} + \frac{\mathbf{p}_2^2}{2M^*} = \frac{p_{z_1}^2}{2M^*} + \frac{p_{z_2}^2}{2M^*} + \frac{\mathbf{P}_{||}^2}{2M} + \frac{\mathbf{p}_{||}^2}{2\mu}. \tag{24}$$

with M and μ being respectively the total effective mass ($2M^*$) and the reduced mass ($M^*/2$). Then writing the Schrödinger equation for the entire wave function Ψ, multiplying by $\phi^*(z_1)\, \phi^*(z_2)$ and integrating over the variables z_1 and z_2, one easily finds:

$$\left[\frac{\mathbf{p}_{||}^2}{2\mu} + \langle V_{\text{eff}}(\mathbf{r}_{||})\rangle\right] \chi(\mathbf{r}_{||}) = E_{\text{dim}}\chi(\mathbf{r}_{||}) \tag{25}$$

where

$$\langle V_{\text{eff}}(\mathbf{r}_{||})\rangle = \int \phi^2(z_1)\, \phi^2(z_2)\, V_{\text{eff}}(\mathbf{r}_1 - \mathbf{r}_2)\, dz_1\, dz_2 \tag{26}$$

According to our perturbation scheme, all the z-dependence has been removed from Eq. ((25). The substrate and the ^{4}He density play an indirect role, through the determination of μ (i.e., M^*) and the z-wave function.

It appears that for all the cases we are interested in (the Andreev state or the substrate state) the z-wave function can be represented to a fairly good approximation by a simple gaussian (characterized by its half-width). In order to explore the sensitivity of the dimer binding energy to the two

most relevant parameters, namely the effective M^* and the width of the ^{3}He wave function, rather than considering only the substrates listed in Table 1, we will give results for various values of M^* and normalized gaussians for $\phi^2(z)$ with various half width.

In the limit of a large half-width, although common perturbation theory cannot be directly applied when looking for the solution of the Schrödinger equation, one can use the Fermi renormalization technique (see [30] and appendix A) to obtain the binding energy with a logarithmic accuracy:

$$|E_{\text{dim}}| \simeq \frac{\hbar^2}{M^* r_0^2} \exp\left(-\frac{M_b^*}{M^*}\frac{L}{|a|}\right) \tag{27}$$

where r_0 is a quantity of the order of the interaction potential range, M_b^* is the effective mass of a ^{3}He quasiparticle in bulk ^{4}He, and L is defined as:

$$\frac{1}{L} = \int |\phi(z)|^4 \, dz \tag{28}$$

Here L is of the order of the half-width, w, and it is a measure of the spatial extension of the z-wave function. The result above is valid only for large values of $L/|a|$ (see Appendix). One can see from Eq. (27) that in this limit the requirements of Sec. 3 are enough to determine the order of magnitude of the dimer binding energy.

In the opposite limit of very localized states—such as those we are primarily interested in—our numerical results show a great sensitivity of the binding energy to the details of the potential (the results for E_{dim} as a function of the half-width for different effective masses are shown on Fig. 7 for V_{eff} and on Fig. 8 for $\tilde{V}_{\text{eff}}$). For instance, for $M^*/m_3 \simeq 3.1$ and $w \simeq 0.5$ Å the binding energies estimated with V_{eff} and $\tilde{V}_{\text{eff}}$ differ from each other by two orders of magnitude. Under these conditions an accurate quantitative prediction would be illusive. We just note that if V_{eff} mimics accurately the exact quasiparticle interaction, it would be very difficult to observe the formation of $(^3\text{He})_2$ bound states in experiment. On the other hand, if the effective potential $\tilde{V}_{\text{eff}}$ can be applied in the case in question, then for a magnesium substrate ($M^*/m_3 = 2.9$ and $w = 0.9$ Å) the dimer binding energy would be $E_{\text{dim}} = -1.1$ mK, which is a reachable temperature with modern experimental techniques. A problem might occur though because the first ^{4}He layer on a Mg substrate could be solid (see the discussion in Sec. 2). The next candidate for dimer formation would then be hydrogen. Using the two potentials designed in Sec. 3 we could not get a reasonable

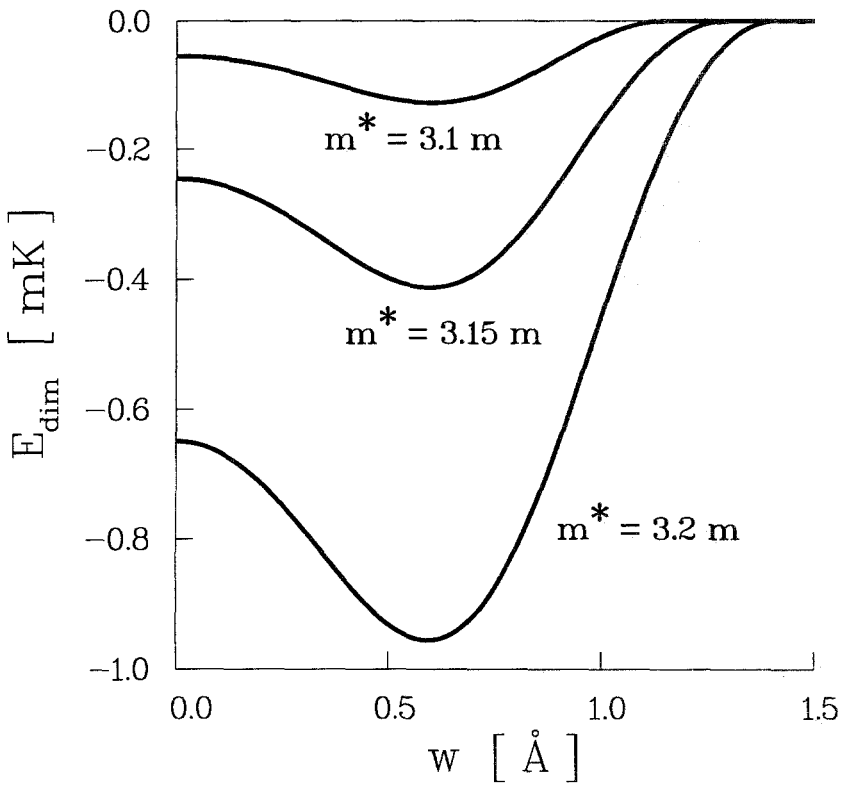

Fig. 7. E_{dim} as a function of w computed with V_{eff} for the effective masses $M^*/m_3 = 3.1$, 3.15 and 3.2.

dimer binding energy, mainly because M^* in this case is not large enough. However, other pseudo-potentials might give a different result.

Note also that the dimer binding energies are very sensitive to the exact value of the s-wave scattering length. This can be seen in the large L (or equivalently large w) limit from Eq. (27). We verified numerically that this is also true for small L: taking the outdated value $a = -1.5$ Å we obtained (using $\tilde{V}_{\mathrm{eff}}$) a dimer binding energy on magnesium $E_{\mathrm{dim}} = -6.3$ mK. Hence experimental information on dimer binding could give valuable insight on the exact value of a.

Although not quantitatively predictive, our study allows us nevertheless to draw a very clear qualitative picture. In highly compressed substrate layers the ^{3}He effective mass is large. This reduces the kinetic energy and favours the creation of $(^3\mathrm{He})_2$ bound states. The small spatial extension of the wave function in these layers is also favorable to the

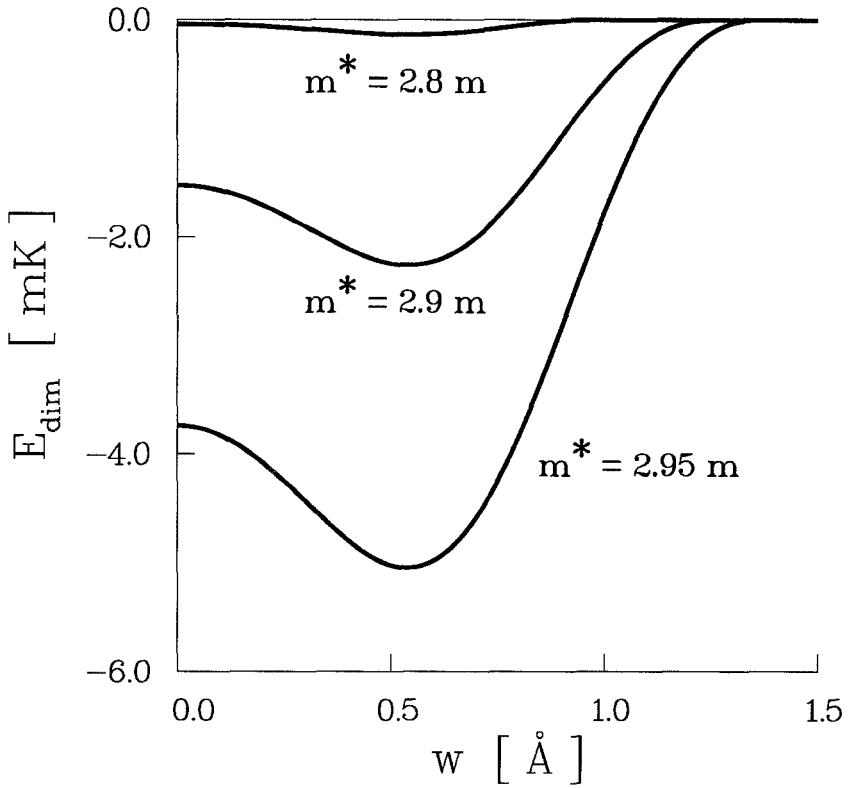

Fig. 8. E_{dim} as a function of w computed with $\tilde{V}_{eff}$ for the effective masses $M^*/m_3 = 2.8$, 2.9 and 2.95. Note the change of energy scale with respect to Fig. 7.

formation of dimers as can be seen from Eq. (27) and Fig. 7 and 8. From these figures one can also see that there is an optimal width of the order of 0.5 Å. It is interesting to note that the more attractive the substrate, the closer one approaches this value (see Table I). The proper way to observe dimers would then be to choose a substrate for which the first ^{4}He layer in close to being solid but still remains liquid.

5. CONCLUDING REMARKS

After having classified various substrates according to their ability to solidify one or two layers of a multilayer helium film, we have concentrated on cases in which helium remains liquid. In addition to the already known Andreev states we have shown that ^{3}He impurities were able to form a new 2D Fermi system near the substrate. After designing a sensible schematic

interaction we have computed the binding energy of $(^3He)_2$ dimers in the limit of small ^3He concentration. We found that for attractive substrates (such as magnesium or hydrogen) there was a reasonable hope to form dimers with sizeable binding energy. Note here that the binding energy of dimers in Andreev surface states is extremely small according to all our estimates, so the observation of $(^3He)_2$ dimers would be a direct consequence of the existence of ^3He substrate states.

In this paper the quantitative calculation of the dimer binding energy was based on a semi-empirical effective interaction and the one-particle wave functions obtained within a density-functional approach. It would be very useful to carry out the appropriate calculations with the help of other theoretical approaches (e.g., Ref. [32]). This would allow a better understanding of the accuracy of the present computations.

We hope that these results will motivate experimental study of the substrate ^3He states as was proposed earlier in [14, 15]. The eventual formation of $(^3He)_2$ dimers would be a very interesting consequence of the existence of these states leading to an amazingly rich phase diagram. An experimentalist could face an extra Kosterlitz-Thouless phase transition, liquefaction of $(^3He)_2$ or polymerization of ^3He, crossover from a Bose gas of dimers to a 2D Fermi fluid (with strong pair correlation) upon increasing the ^3He concentration, etc. [8, 9, 33, 34, 35, 36]. The dimer binding energy is a cornerstone characteristic of all these phenomena which are exciting objectives for experimental and theoretical studies.

A natural continuation of the present work would be to study the binding of two dimensional clusters of ^3He atoms. Although Fermi statistics favours droplets with even numbers of ^3He atoms, there might be no upper limit for N, and our results could be a hint of the existence of a 2D liquid phase of ^3He. On the basis of a regular arrangement in two dimensions (with 6 nearest neighbours per atom) we estimate the saturation energy of the liquid phase to be (in the most favourable case) of the order of 5 to 6 mK. This is to be related to the recent finding of Brami *et al.* [37] whose variational results lead to propose at low temperature a new "self-condensed" fluid phase for pure ^3He films on graphite. As the presence of ^4He favours the formation of ^3He dimers it could also favour the formation of a liquid phase.

APPENDIX A

In this appendix we derive the expression (27) for the dimer binding energy E_{dim} using the Fermi renormalization technique (see [30]). According to this method we introduce a weak two-particle pseudo-potential

$V_f(r)$ which is assumed to meet the perturbation theory criterion. Let us emphasize that such an pseudo-potential has nothing to do with the interaction between quasiparticles which, indeed, cannot be treated in terms of a perturbation theory at all.

The pseudo-potential V_f is supposed to result in the true scattering amplitude when calculated within the Born approximation:

$$a = \frac{M_b^*}{4\pi\hbar^2} \int V_f(r)\, d^3r \tag{A1}$$

where M_b^* is the effective mass of a ^{3}He quasiparticle in bulk ^{4}He ($M_b^* = 2.38\, m_3$). The idea of the method is to carry out all calculations in the framework of a perturbation theory for V_f and then to express the final formulae through the true s-wave scattering length a only by means of the renormalization (A1). Thus the method works while all obtained expressions contain the pseudopotential V_f only in the integral form (A1).

The solution of the Schrödinger equation, i.e., of Eq. (25) with V_f replacing V_{eff}, may be expressed in the form (see e.g., Ref. [10, 31])

$$E_{\text{dim}} \simeq -\frac{\hbar^2}{2\mu r_0^2} \exp\left[-\frac{\hbar^2}{\mu} \left| \int_0^\infty \langle V_f \rangle\, \rho\, d\rho \right|^{-1} \right] \tag{A2}$$

where $r_0 \sim |a|$ is of the order of the interaction range and $\langle V_f \rangle$ is defined by (26) with V_f replacing V_{eff}. Let us recall once again that the pseudopotential V_f is assumed to meet the criterion of a perturbation theory: for instance the integral entering Eq. (A2) should converge. Denoting this integral as I one can write:

$$I = \int_0^\infty \langle V_f \rangle\, \rho\, d\rho = \int V_f(\sqrt{\rho^2 + z^2})\, F(z)\, \rho\, d\rho\, dz \tag{A3}$$

where

$$F(z) = \int |\phi(t - z/2)|^2\, |\phi(t + z/2)|^2\, dt \tag{A4}$$

Let the quantity w be a characteristic localization range in the z-direction for the wave function ϕ (w describes the half-width introduced in Sec. 4). If the localization length is sufficiently large, $w \gg r_0$, one can easily find that

$$I = \frac{1}{2\pi L} \int V_f(r)\, d^3r \qquad \text{with} \quad \frac{1}{L} \equiv F(0) = \int |\phi(t)|^4\, dt \tag{A5}$$

Clearly L is of the same order as w (if ϕ^2 is a normalized gaussian of half-width w, then $L = w\sqrt{\pi/\ln 4}$). Combining Eq. (A5) and the renormalization relation (A1) yields:

$$E_{\text{dim}} \simeq -\frac{\hbar^2}{M^* r_0^2} \exp\left[-\frac{M_b^*}{M^*}\frac{L}{|a|}\right] \tag{A6}$$

In (A6) we have replaced the reduced mass by its value for the state $\phi(z)$ considered: $\mu = M^*/2$. We see that the binding energy is expressed in terms of the true scattering amplitude and does not contain a pseudopotential in any explicit form. Thus using the Fermi method is completely justified in the limiting case $w \gg r_0$. Note, however, that it is difficult to determine exactly the quantity r_0 (see [31]) which could, in general, be pseudo-potential dependent. On the other hand, its order of magnitude is known ($r_0 \sim |a|$) and, in fact, it does not enter the exponential factor which determines the dominant behavior of E_{dim}.

In the limiting case $w \ll r_0$ the integral I obviously reduces to

$$I = \int V_f(\rho)\, \rho\, d\rho \tag{A7}$$

and the binding energy explicitly depends on what kind of a pseudopotential is chosen. It means that the renormalization method is no longer valid and the 2D Schrödinger equation with the real interaction potential should be solved to find the binding energy. In this paper we have chosen to perform the calculation of E_{dim} by means of semi-empirical pseudopotentials which gave rise to reasonable estimates for quantities measured in experiment (see Sec. 2).

ACKNOWLEDGMENTS

We thank M. W. Cole and M. Devaux for fruitful discussions. This research was supported in part by the Deutsche Forschungsgemeinschaft (BA 1229/4-1). One of the authors (E. B.) greatly appreciates the warm hospitality extended to him at the Pennsylvania State University where part of this work was done under the NSF Grant DMR-9022681.

REFERENCES

1. G. Baym and C. Pethick, in *The Physics of Liquid and Solid Helium*, K. H. Bennemann and J. B. Keterson, eds. (Wiley, N.Y. 1978), Vol. II.
2. L. D. Landau and I. Pomeranchuck, *Dokl. Akad. Nauk SSSR* **59**, 669 (1948).
3. J. Bardeen, G. Baym, and D. Pines, *Phys. Rev.* **156**, 207 (1967).

4. E. P. Bashkin, *Soviet Phys. JETP Lett.* **25**, 1 (1977); *Soviet Phys. JETP.* **46**, 972 (1977).
5. E. P. Bashkin and A. E. Meyerovich, *Adv. Phys.* **30**, 1 (1981).
6. J. R. Owers-Bradley, D. R. Wightman, A. Child, A. Bedford, and R. M. Bowley, *J. Low Temp. Phys.* **88**, 221 (1988).
7. D. Candela, D. R. McAllaster, and L.-J. Wei, *Phys. Rev. B* **44**, 7510 (1991).
8. E. P. Bashkin, *Soviet Phys. JETP* **51**, 181 (1980).
9. E. P. Bashkin, in *Recent Progress in Many-Body Theory* **3**, Ed. by C. Campbell, B. Clements, E. Krotscheck and T. Ainsworth, (Plenum Press, 1992).
10. L. D. Landau and E. M. Lifshitz, *Quantum Mechanics* (Pergamon, Oxford 1977).
11. A. F. Andreev, *Soviet Phys. JETP* **23**, 938 (1967).
12. D. O. Edwards and W. F. Saam, in *Progress in Low Temperature Physics*, D. F. Brewer, ed. (North-Holland, Amsterdam 1978), Vol. VII A, p. 283.
13. N. Pavloff and J. Treiner, *J. Low Temp. Phys.* **83**, 15 (1991).
14. N. Pavloff and J. Treiner, *J. Low Temp. Phys.* **83**, 331 (1991).
15. J. Treiner, *J. Low Temp. Phys.* **91**, 1 (1993).
16. E. Cheng, M. W. Cole, W. Saam, and J. Treiner, *Phys. Rev. Lett.* **67**, 1007 (1991).
17. A. F. Andreev, in *Quantum Theory of Solids*, edited by I. M. Lifshitz (MIR, Moscow 1982), p. 11.
18. E. Cheng, M. W. Cole, W. F. Saam, and J. Treiner, *Phys. Rev. B* **46**, 13967 (1992).
19. G. Vidali, G. Ihm, H. Y. Kim, and M. W. Cole, *Surf. Sci. Rep.* **12**, 133 (1991).
20. E. Cheng, M. W. Cole, W. Saam, and J. Treiner, *J. Low Temp. Phys.* **91**, 10 (1993).
21. F. Dalfovo and S. Stringari, *Phys. Scr.* **38**, 204 (1988).
22. I. B. Mantz and D. O. Edwards, *Phys. Rev. B* **20**, 4518 (1979).
23. D. O. Edwards and W. F. Saam, in *Progress in Low Temperature Physics*, D. F. Brewer ed. (North Holland, Amsterdam, 1978), Vol. VII A, p. 283.
24. F. Dalfovo, *Z. Phys. D* **14**, 263 (1989).
25. R. B. Hallock, *Can. J. Phys.* **65**, 1517 (1987).
26. E. Rolley, S. Balibar, C. Guthmann, and P. Nozières, preprint 1994.
27. L. J. Campbell, *Phys. Rev. Lett.* **19**, 156 (1967).
28. R. A. Aziz, V. P. S. Nain, J. S. Carley, W. L. Taylor, and G. T. McConville, *J. Chem. Phys.* **70**, 4330 (1979).
29. J. C. Owen, *Phys. Rev. Lett.* **47**, 586 (1981).
30. E. M. Lifshitz and L. P. Pitaevskii, *Statistical Physics*, Part 2, (Pergamon 1980).
31. E. N. Economou, *Green's Functions in Quantum Physics*, Springer Series in Solid-State Sciences **7** (Springer-Verlag, 1983).
32. E. Krotscheck, M. Saarela, and J. L. Epstein, *Phys. Rev. Lett.* **61**, 1278 (1988); **64**, 427 (1990).
33. A. J. Legget, in *Modern Trends in the Theory of Condensed Matter*, edited by A. Pekalski and R. Przystawa (Springer-Verlag, Berlin, 1980), p. 13; *J. Phys.* (Paris), **41**, C7-19 (1980).
34. K. Miyake, *Progr. Theor. Phys.* **69**, 1794 (1983).
35. P. Nozières and S. Schmitt-Rink, *J. Low Temp. Phys.* **59**, 195 (1985).
36. E. Østgaard and E. Bashkin, *Physica B* **178**, 134 (1992).
37. B. Brami, F. Joly, and C. Lhuillier, *J. Low. Phys.* **94**, 63 (1994).